Biomass Conversion and Biorefinery (2022) 12:2377–2387
https://doi.org/10.1007/s13399-020-00766-2

ORIGINAL ARTICLE

Structural changes of waste biomass induced by alkaline treatment: the effect on crystallinity and thermal properties

Tatjana Šoštarić[1] · Marija Petrović[1] · Jovica Stojanović[1] · Marija Marković[1] · Jelena Avdalović[2] · Ahmad Hosseini-Bandegharaei[3,4] · Zorica Lopičić[1]

Received: 26 February 2020 / Revised: 5 May 2020 / Accepted: 8 May 2020 / Published online: 22 May 2020

Abstract

A low-cost waste biomass generated from a food industry, apricot shells, was subjected to alkali modification in order to compare morphology, crystalline structure and thermal stability of native and modified biomass, accompanied by their cellulose-rich fractions. The surface morphology and structure of compared samples were analysed by the scanning electron microscopy (SEM) and mercury porosimetry. Furthermore, Fourier transform infrared spectroscopy (FTIR), X-ray diffraction (XRD) and thermal analysis (TG/DTA) were applied. The results have shown that after alkaline treatment, inter- and intra-particle porosity in the material rises, resulting in increase of the total surface area. The XRD diffractograms showed that crystallinity index increased together with crystallite size, suggesting that modified sample has more ordered crystalline structure than native sample (also confirmed by the FTIR analysis). Although the cellulose-rich fraction extracted from the alkali-modified sample showed higher thermal stability, the overall thermal analysis revealed that alkali-modified biomass has lower thermal stability than the native sample. This indicates that this type of modification will improve the fuel properties of this lignocellulosic biomass and imply its possible application in energy recovery process.

Keywords Low-cost biomaterials · Apricot shells · Modification · Surface, characterization

1 Introduction

The main characteristic of residual lignocelluloses biomasses is a large annual generation rate and a low economic value [1]. Apricot stones generated as a by-product from the food industry production are good examples of such biomass. Apricots are significant and valuable fruit crops in Serbia, with annual production in 2017 of 41,320 tons (http://publikacije.stat.gov.rs/G2018/pdf/G20189085.pdf). This amount of fresh fruits generates significant amount of solid, biodegradable waste: approximately 8000 tons per year. Apricot endocarp (also known as apricot shell) is a lignocellulose (LC) material based predominantly on cellulose, hemicellulose and lignin. Although apricot kernels could be used in food or pharmaceutical industry [2], apricot shells usually end up at landfill or are burned.

Food processing and food waste management in Serbia are very limited, and unfortunately most of this valuable, low-cost resource ends up in open landfills. In Serbia 770,000 tons of food are wasted annually, and currently less than 10% of this biodegradable waste are recycled. According to German Agency for International Cooperation report "Climate Sensitive Waste Management Project in Serbia" (https://germancooperation.rs), estimation is that by diverting food waste from landfills, savings of 580 kg CO_2eq per ton can be made. Also, the dumping of biodegradable waste at open landfills causes a significant amount of greenhouse gas CH_4 emission, which has more than 28 global warming potential (GWP) compared with CO_2 (1GWP).

In order to find an economical usage of LC waste biomass in environmental science and technology, many authors have

✉ Tatjana Šoštarić
t.sostaric@itnms.ac.rs

[1] Institute for Technology of Nuclear and Other Mineral Raw Materials, Franchet d'Esperey 86, Belgrade 11000, Serbia

[2] Institute for Chemistry, Technology and Metallurgy, University of Belgrade, Njegoševa 12, Belgrade 11000, Serbia

[3] Environment Health Engineering Department & Social Determinants of Health Research Centre, Gonabad University of Medical Sciences, Gonabad, Iran

[4] Department of Engineering, Kashmar Branch, Islamic Azad University, PO Box 161, Kashmar, Iran

published papers which are mostly based on the sorption properties of this kind of materials. In most of the papers, biosorption capacity has been improved by exploiting different types of modification. For example, Ronda et al. [3] showed that chemically modified olive stones have significantly improved sorption performance toward Pb(II) ions, while Lopičić et al. [4] applied mechanical activation on peach shells and showed that this type of treatment has an effect on Cu(II) kinetic removal efficiency. Turk Sekulić et al. [5] used apricots stones as a precursor for preparation of biochars in order to make a sorbent for removal of Pb(II) and Cr(III) ions from wastewaters. Some authors used activated carbon made from plum stones to remove heavy metals ions and chlorophenols from contaminated waters [6]. Despite the numerous studies concerning this topic, there is still lack of data on structural changes induced by various types of treatments.

In our previous paper [7], we had investigated the effect of alkali treatment on apricot shells for heavy metal removal and gained enhanced biosorption capacity. In opposite, Carvalho and Virgens [8] obtained results which indicated that inorganic alkali modification of fruit peel of *Pachira aquatica* Aubl. decreased sorption capacity of native material toward Cd by more than 60%. It is well known that treatment effects depend on the physical structure and chemical composition of the material, as well as on the treatment conditions, which indicates that each material should be investigated in order to establish its properties. Regarding the papers related on sorption characteristics, alkali treatment is mainly reflected on sorption mechanism, but it is also affecting morphology of the material which reflects on mass and heat transfer.

Having in minds all of the mentioned, we have decided to get insights into the influence of the alkaline treatment on chemical/crystalline structure and thermal stability of lignocellulosic biomass. Therefore, in this paper, we have described the effect of the alkaline treatment on apricot shells' biomass by studying the obtained changes in crystalline structure of treated biomass and its extracted cellulose-rich fraction. The thermal stability of modified sample was also investigated in order to give direction for further possibility of application of treated sample as a fuel. The changes were examined by SEM, mercury porosimetry, Fourier transform infrared spectroscopy (FTIR), X-ray diffraction (XRD) and thermal analysis (TG/DTA).

To the best of our knowledge, no studies, to date, have reported the effect of alkaline treatment on the structure of apricot shells (except for the purpose of sorption properties enhancement). This paper is focused on LC characteristics that can provide a deeper analysis of the changes induced by alkaline treatment, and which suggest its possible reuse in energy recovery and environmental processes.

2 Materials and methods

2.1 Materials

Apricot stones were collected from a local Juice Factory in Aleksandrovac, Serbia. The apricot shells were manually separated from seeds. The shells were washed and dried at 50 °C until the mass remained constant; then they were grinded (KHD Humboldt Wedag AG, Germany) and sieved (particles less than 1.0 mm were used for experiments). The obtained sample was marked as SH.

Furthermore, 50 g of the obtained SH sample was alkali treated with 1.0 L of 1.0 mol/L NaOH. The reaction mixture was stirred on a magnetic stirrer at 250 rpm for 3 h at room temperature. In order to remove excess base from the sample, the mixture was filtered under vacuum using a Buchner funnel and repeatedly washed with distilled water until stable pH value was observed. Afterward residue was dried at 50 °C until reaching a constant mass. Alkali treated powder was labelled as SHM.

2.2 Methods

The methods for extraction of cellulose and lignin rich fractions were descripted in detail elsewhere [7]. Sample surface was scanned by using SEM model JSM-6610 LV (Jeol, Japan), after the samples' gold coating. Mercury intrusion porosimetry was used for determination of samples porosity. For that purpose, Pascal 140/440 (Thermo Scientific) was used. FTIR spectres were obtained by using the Thermo Nicolet 6700 spectrometer in the spectral range of 4000–400 cm^{-1}, at resolution of 4 cm^{-1} in KBr mode. Thermal analysis (DTA/TG) was done in air atmosphere on a Netzsch STA 409 EP in the temperature range from 20 to 1000 °C at heating rate of 10 °C min^{-1}. The XRD patterns were obtained on a Philips PW-1710 automated diffractometer using a Cu tube operated at 40 kV and 30 mA. The instrument was equipped with a diffracted beam curved graphite monochromator and an Xe-filled proportional counter. The diffraction data were collected in 2θ Bragg angle range from 4° to 65°, counting for 0.5 at every 0.02° step. Table 1 summarizes all equations that were used to evaluation of changes in crystalline structure before and after alkaline treatment.

3 Results and discussion

Apricot shell (endocarp) provides necessary seed protection against unfavourable environmental factors (mechanical, chemical and microbial stresses), due to its complex structure and specific chemical composition. Previous research have shown that the main components of apricot endocarp are cellulose (55.23%), lignin (22.72%) and hemicellulose (19.23%)

Table 1 Equations used for evaluation of changes in crystalline structure

Equation	Parameter	Ref
$CrI = \frac{I_{002}-I_{am}}{I_{002}} \times 100\%$	CrI: crystalline index I_{002}: cellulose crystalline peak intensity at 22.5° 2θ I_{am}: amorphous peak intensity at 18.5° 2θ	[9]
$D_{002} = \frac{k\times\lambda}{\beta\cos\theta}$	D_{002}: crystalline size of (002) plane k: Scherrer constant (0.94) λ: X-ray wavelength (0.154 nm) β: full width at half maximum of (002) peak θ: diffraction angle of (002) plane	[10]
$HBI = \frac{A_{3345}}{A_{1320}}$	HBI: hydrogen bond intensity A_{3345}: absorbance peaks at 3345 cm^{-1} A_{1320}: absorbance peaks at 1320 cm^{-1}	[11]
$TCI = \frac{A_{1372}}{A_{2900}}$	TCI: total crystalline index A_{1372}: absorbance peaks at 1372 cm^{-1} A_{2900}: absorbance peaks at 2900 cm^{-1}	[11]
$LOI = \frac{A_{1429}}{A_{897}}$	LOI: lateral order index A_{1429}: absorbance peaks at 1429 cm^{-1} A_{897}: absorbance peaks at 897 cm^{-1}	[11]
$E_H = \frac{1V_o-V}{k\ V_o}$	E_H: hydrogen bond energy V_0: free OH group absorbance at 3650 cm^{-1} V: bonded OH group absorbance k: the constant ($1/k = 2.625 \times 102$ kJ)	[11]
$\Delta V(cm^{-1}) = 4430(2.84 - R)\quad \Delta V = V_0 - V$	R: the hydrogen bond distances V_0: the monomeric OH stretching vibration at 3600 cm^{-1} V: the stretching vibration observed in FTIR spectrum of the sample	[11]

[7]. The mentioned constituents have very close interactions with each other, making the unique structure of endocarp. Alkaline treatment changes not only morphological properties (Fig. 1) but also the chemical characteristics of native apricot shells, due to a hemicellulose hydrolysis and lignin depolymerisation [7]. Alkali treatment in SHM promoted

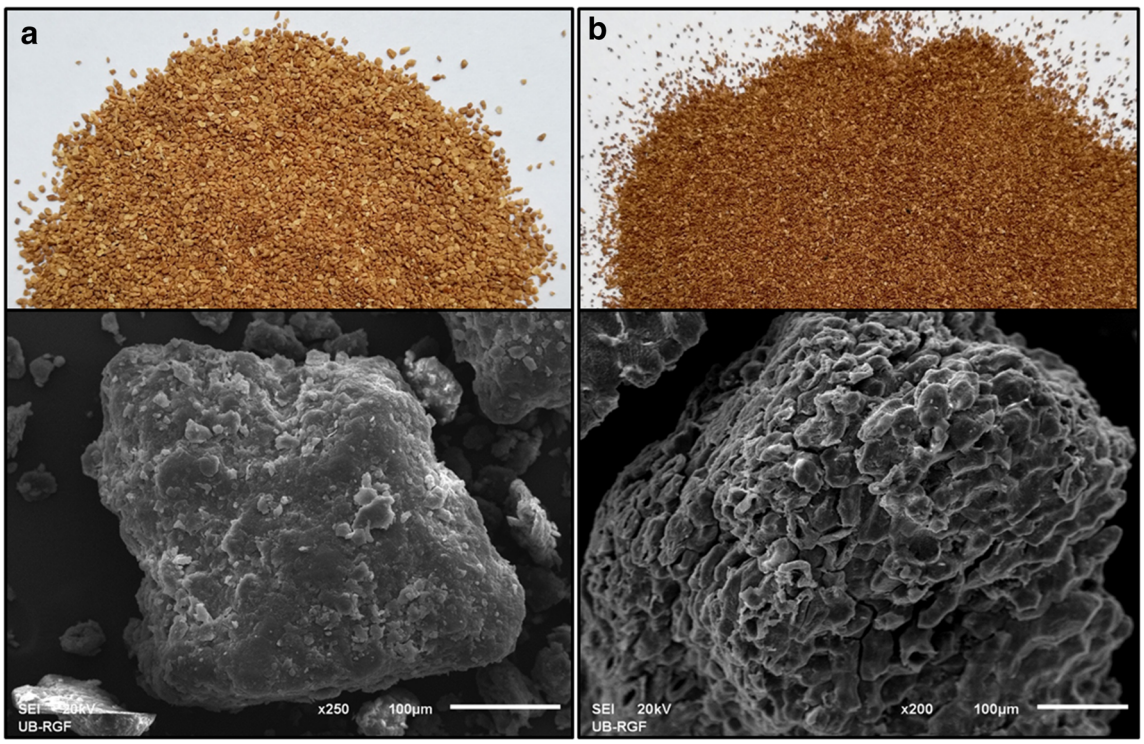

Fig. 1 Morphological changes of **a** untreated SH and **b** alkali treated apricot shells SHM

roughness and irregularities on the surface of the natural material (SH), allowing the particles to aggregate less than in the starting sample. However, low-temperature alkali treatment results in a very limited process of lignin degradation or fragmentation, due to the presence of chemical groups which are very resistant to chemical agents (e.g. C–C linkages or aromatic groups) [12]. Although hemicellulose is soluble in alkaline solutions, it cannot be completely removed, due to the stable hydrogen bonding between hemicellulose and cellulose fibrils [13]. In our previous paper we showed that alkaline treatment decreases amorphous constituents hemicellulose and lignin by almost 80% and 10%, respectively, as well as increases the cellulose content [7].

3.1 Textural characteristics of SH and SHM

Textural characteristics of porous materials could be determined by various methods, and the choice of appropriate method depends on material nature and its pore size. Mercury porosimetry was chosen for this type of biomass, because the Brunauer-Emmett-Teller (BET) method is more suitable for meso- and microporous materials, while mercury porosimetry is more suitable for macroporous materials [14]. The choice of the method was justified by the results obtained from SEM analysis which revealed that sample's particles predominantly consist of macropores (approximately 1 μm in diameter). Mercury porosimetry gives information not only about the volume and the pore distribution in particle interior (intra particle porosity) but also describes inter-particle porosity-free space between the particles. Due to the increase of the available surface area, it is ideal that the both types of porosity are presented in material. We showed that alkaline treatment causes an increase in porosity (by 20%), total pore volume (by 24%), specific surface area (by 33%) and average pore diameter (by 20%) [7], as well as that the inter-particle volume is 26% higher in SHM than in SH (171 and 136 mm^3/g, respectively—Fig. 2). In Fig. 2, it is evident that the fraction of the smallest (> 100 μm) and the biggest (500–800 μm) particles slightly decreased, while the most numerous average size particle fraction (100–500 μm) slightly increased as a consequence of chemical modification. The obtained results of this analysis confirmed the presence of both porosity types in SHM.

3.2 XRD patterns

In order to attain more profound examination of the alkaline treatment effect on crystalline structure of SH and its cellulose-rich fraction, further investigations were performed. Diffractograms of SH and SHM in Fig. 3a show the differences in their crystal structure.

Figure 3a shows that both samples have peak characteristic for cellulose I (card No. PDF-203-0289) located on $2\theta \approx 14^\circ$, 16°, 23° and 35° which are ascribed to the (101), (10$\bar{1}$), (002) and (040) crystallographic plane reflection, respectively [15, 16]. According to literature [17], the X-ray diffractograms of amorphous solids and lattice distortion show a wide peak, while solids with crystalline structure have sharper peaks indicating larger crystallites. Diffractogram of untreated sample SH shows two peaks: sharper peak at $2\theta \approx 23^\circ$ corresponds to the (002) crystallographic plane of cellulose I and another wider peak at $2\theta \approx 16^\circ$ corresponds to the (10$\bar{1}$) crystallographic plane of cellulose I (referring amorphous phase of SH). This is in accordance with high content of hemicellulose and lignin which contributes to amorphous phase [18]. It is observed from Fig. 3a that alkali treatment has no effect on the peaks' position, but it has a noticeable effect on the shape and intensity of the peaks in treated sample. The apparent peaks in diffractogram of SHM are sharper and larger than in diffractogram of SH, which indicates that after alkaline treatment, certain increase in crystallinity has been occurred. The calculated values of the crystallinity index *CrI*, according to Eq. (1), are 39% and 47% for SH and SHM samples, respectively. These results are comparable with very similar natural lignocellulosic biomass such as peach shells (39.2%) [4]. Also, after chemical treatment, crystallite size (D_{002}) according to Eq. (2) increased from 24 to 43 Å for SH and SHM, respectively. Increase of crystallite size might be associated with decrease of amorphous region, too [19]. These results confirmed that the amorphous regions of the cellulose are "attacked" throughout the alkali treatment, which led to a reduction of the amorphous region, and increase of the crystallinity and/or a reorganization of the crystalline regions. Similar results were obtained by Carvalho and Virgens [8] who confirmed that alkali treatment also modified the structure of the solid biomass, resulting in greater crystallinity, from 41.7 for native biomass sample up to 53% for alkali modified.

According to Borysiak and Doczekalska [20], alkaline treatment removes hemicellulose and impurities and interfibrillary spaces in lignocellulosic fibres become less dense and rigid; therefore, cellulose micro-fibrils rearrange themselves to have better chain orientation and packing, which leads to an increase of fibre strength. Alkaline treatment (depends on alkali concentration), besides the effect on cellulose crystallinity, can also transform the crystalline structure of cellulose to different allomorphs with different unit cell dimension packing arrangements and relationships between hydrogen bonds [16]. In accordance with that, the X-ray diffraction patterns of cellulose-rich fraction isolated from SHM (Fig. 3b) show that alkali treatment not only has a noticeable effect on intensity of the main peak in treated sample, but it shows that some peaks become slightly more defined upon this chemical treatment: $2\theta = 12.0^\circ$ and 20° assigned to the (101) and (10$\bar{1}$) lattice planes of cellulose II, respectively [14, 15]. These discrete peaks might be indicators of the early

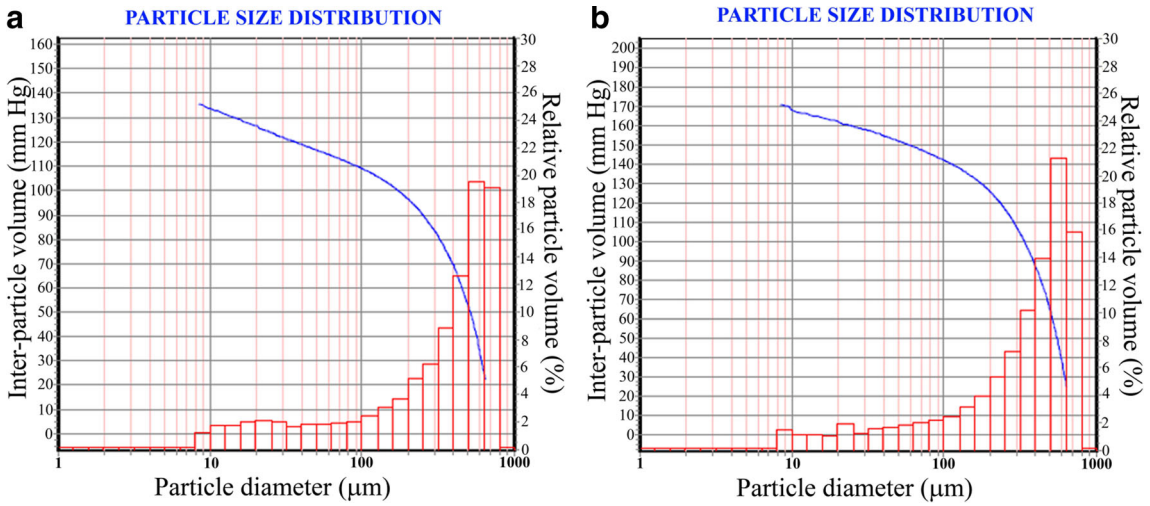

Fig. 2 Inter-particle volume and particle size distribution: SH (**a**) and SHM (**b**)

beginning of transformation of cellulose I into cellulose II, since this sample had been alkali-treated twice: during process of modification and afterwards during the cellulose isolation procedure (with 17.5% aqueous NaOH solution).

It is well known that the conversion of cellulose I to cellulose II can be performed by using of sodium hydroxide (process of mercerization). This process affects microfibers; they become swollen with disrupted connections and orientation [21]. The chains in cellulose I are parallel and mainly linked by van der Waals interactions, while the chains of cellulose II are antiparallel, and consequently the number of hydrogen bonds between molecular layers are higher. Cellulose II is thermodynamically more stable because hydrogen bindings are much stronger than van der Waals bindings [22]. Chemically, allomorph cellulose II has a higher chemical reactivity in comparison with cellulose I (e.g. the sorption capacity of cellulose II is greater) [23]. Its chemical reactivity depends on the location of the hydroxyl groups on the anhydroglucose unit. This cannot be generalized because different conditions and interactions affect the reactivity of the groups.

3.3 Fourier transform infrared spectroscopy (FTIR)

In order to show source of peaks in SH and SHM, the FTIR spectra of extracted cellulose and lignin fractions are presented in the Fig. 4.

Two distinctive regions of FTIR spectra are noticeable: the region from 3700 to 2800 cm^{-1} corresponding to -OH and -CH stretching vibration and "finger print" region from 1800 to 800 cm^{-1} corresponding to stretching vibration of various chemical groups in lignocellulosic materials. The broad peak in the range from 3000 to 3600 cm^{-1} is corresponding to stretching vibration of OH groups in cellulose, hemicellulose and lignin [24]. Changes in the peak intensity in this region indicate the disturbances of intermolecular and intramolecular hydrogen bonds in cellulose [25]. The disappearance of absorption band at 1742 cm^{-1} after alkaline treatment in SH sample was noted. Similar findings were obtained by Lehto et al. [26] who alkali treated wood samples (birch and pine). This band corresponds to C=O stretching vibration of carbonyl and acetyl groups in the xylan and to chemical groups present in lignin (p-coumaric acids of lignin) [27]. The

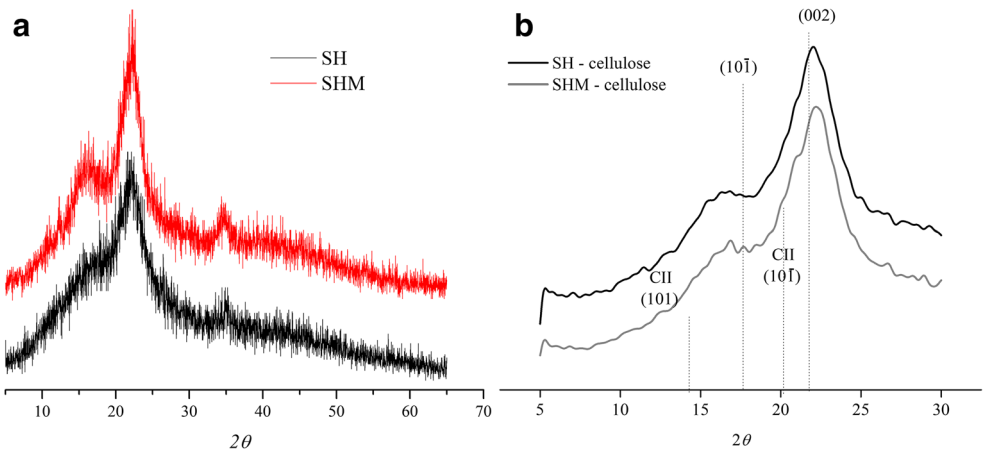

Fig. 3 Diffractograms of SH and SHM (**a**) and isolated cellulose-rich fraction from SH and SHM (**b**)

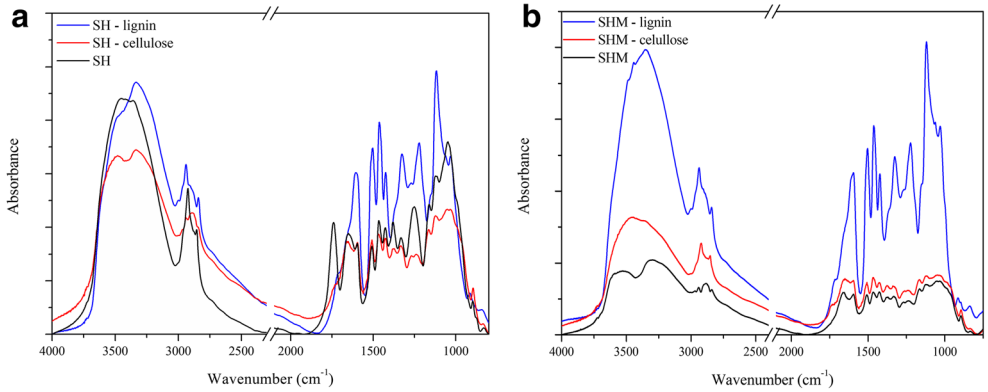

Fig. 4 FTIR spectra of isolated cellulose and lignin from SH and SHM compared with the starting sample

reduction of intensity of the absorption peak observed in SH at 1252 cm^{-1} assigned to asymmetric C–C–O stretching from carbon in aromatic rings was noticed as well [28]. Apparently, this band in natural biomass sample (SH) overlapped two bands: 1270 and 1226 cm^{-1} assigned to C–O stretching vibration in guaiacol rings and syringol rings, respectively [29]. Dominant peak in lignin-rich fraction spectra at 1600 cm^{-1} corresponding to C=C aromatic skeletal vibration in lignin also overlaps two bands at 1652 and 1597 cm^{-1} in SH. Barely visible shoulder at 1650 cm^{-1} in lignin-rich fraction indicates that the conjugated carbonyl groups present in lignin were cleaved during the extraction [30]. Next, three bands at around 1510, 1466 and 1426 cm^{-1} (due to C=C aromatic skeletal vibrations, C–H deformation and vibration in phenylene ring, respectively) dominates in lignin spectra of both material. In spectra of isolated lignin, peak at 1120 cm^{-1} gives more intense adsorption band, due to aromatic C–H in-plane deformation in lignin [31]. In order to identify the chemical groups originating from lignin (L), hemicellulose (HC) or cellulose (C), wavenumbers of the bands are presented and marked in the Table 2.

It is well known that the presence of the hydrogen bonds has a significant influence on the mechanical properties of lignocellulosic materials. The closer cellulose chains result in the stronger interactions between them, leading to stronger hydrogen bonds and more compact packing of cellulose chains. Thus, the fibres become mechanically and thermally more stable [38]. FTIR has been widely used in order to get more profound understanding of the hydrogen bond nature, by analysing intensities and positions of the OH stretching vibration peak [39]. As can be seen from Fig. 4, the intensity of SHM peaks decreased after alkaline modification. Since the reduction in hemicellulose and lignin content after modification has been occurred, the reduction of absorbance of this region could be an indication of more organized cellulose in SHM sample [36].

Furthermore, Fig. 5 shows a comparison of extracted cellulose from SH and SHM. Results in Fig. 5 revealed that the peak of the OH vibration in cellulose-rich fraction isolated from SHM becomes red-shifted (from 3482 to 3457 cm^{-1}) and its intensity slightly decreased, suggesting increase of the number of hydrogen bond interactions [40].

Summarized differences between SH and SHM are presented in Table 3. The energy of hydrogen bonds is higher in SHM than in SH, indicating higher crystallinity and higher presence of hydrogen bonds [11]. This is in accordance with the results of XRD analysis (higher *CrI* and D_{002} in SHM). Also, due to higher *HBI* value in SHM, it can be concluded that this sample contains more cellulose chains in highly organized form. Alkaline modified sample SHM possibly has stronger hydrogen bonds between chains and more packed structure of cellulose, which is in accordance with its lower hydrogen bond distances (*R*).

In spite of the fact that increase in crystallinity leads to less reactive samples, results from our previous paper revealed that alkaline treatment significantly improved the sorption performance of modified sample SHM in comparison with native sample SH toward the investigated heavy metals. In comparison with the native sample SH, biosorption capacity of SHM was increased by 154, 61 and 90% for Cu(II), Zn(II) and Pb(II) ions, respectively [7]. Similar results were obtained when peach shells were subjected to mechanical treatment: the obtained less reactive sample (with higher crystallinity) had a better sorption performance toward Cu(II) ions in comparison with more reactive sample [4]. A possible explanation could be related to the change of dominant sorption mechanism: alkali treatment enhanced cation exchange capacity (CEC) five times which enables the ion exchange as the main sorption mechanism [7]. Beside the changes in sorption mechanisms, the reason for sorption increase also could be found in textural characteristics of chemically modified sample: in comparison with SH, SHM sample has higher porosity, total pore volume and average pore diameter, as well as higher value of the specific surface area. It is well known that all mentioned textural characteristics affect mass transfer of ions within the particles toward active sites [41].

Table 2 Wavenumber of the bands obtained from different FTIR spectra

SH	SHM	SH cellulose	SHM cellulose	SH lignin	SHM lignin	Peaks assignments	Ref
3452 3353	3529 3299	3482 3336	3457 3360	3446 3336	3444 3351	O–H str. (C)	[32]
2924 2854	2942 2887	2940 2889	2923 2853	2940 2844	2938 2844	$C–H_n$ str.	[32]
1742						C=O str. (HC)	[33]
1652	1661	1659	1651	Sh.	Sh.	C=O str. (L)	[31, 32]
1597 1509	1597 1509	1597 1508	1597 1507	1606 1505	1596 1507	C=C arom. skeletal vib. (L)	[30, 32]
1466	1468	1468	1468	1464	1464	C–H def. (HC, L)	[28]
1426 1380	1426 1371	1427 1380	1428 1378	1425	1426	C–H def.(C, L) C–H bending (C_I and C_{II}; HC)	[33, 34]
1331	1333	1332	1340	1326	1329	C–H (C); C–O (L)	[28]
1252	1270	1268	1262	1270	1270	C–O str. vib. in guaiacol rings (L)	[27]
	1238	1238	1238	1221	1226	C–O str. vib. in syringol rings (L)	[35]
1161	1165	1165	1167			C–O–C asym. str. vib. (C_I and C_{II})	[36]
1124	1124	1122	1120	1118	1120	Glucose ring str. (C), C–H def. (L)	[31]
1050	1054	1053	1047			C–O str.; C–H vib. (C)	[37]
	1034	1033	1035	1032 913	1030 916	C–O str. (C, L) C–H def. (L)	[31]
897 830	895 836	895 835	895 834	843	839	C–H def (C) C–H def. (L)	[31]

3.4 Thermal analysis

Thermal analyses are used for the study of thermal behaviour of various materials to provide information about thermal stability and decomposition process. Thermal decomposition of lignocellulosic materials such as apricot shells depends on its individual components such as cellulose, lignin and hemicellulose and on individual decomposition behaviour [42]. In order to investigate the effects of modification on the combusting characteristics of raw material, the thermal analyses were performed. Figure 6 shows the results obtained from analysis of the mass loss (TG), derivate of mass loss (DTG) and differential thermal analysis (DTA) obtained during combustion of SH and SHM samples, respectively.

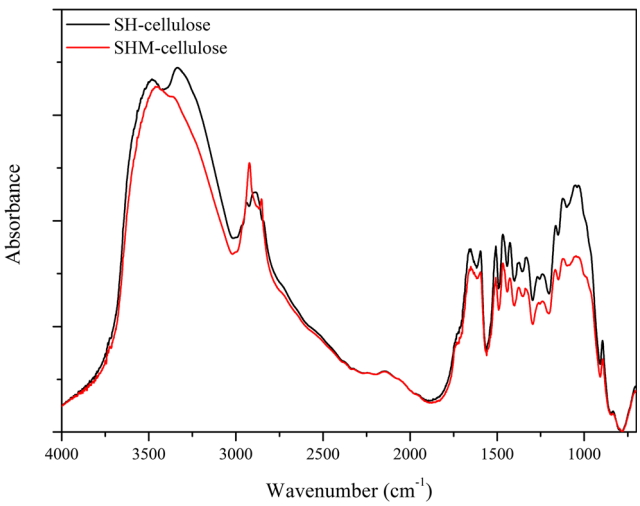

Fig. 5 FTIR spectra of SH and SHM isolated cellulose-rich fraction

The shapes of SH and SHM TG curves are very similar to the other comparable lignocellulosic materials [43], describing the decomposition process through several overlapping stages. The initial mass loss in interval from 25 to 150 °C corresponds mostly to evaporation of physically bounded

Table 3 Energy of the hydrogen bonds, hydrogen bond distance, TCI, LOI and HBI ratios obtained for SH and SHM

	CrI (%)	D_{002} (Å)	HBI	LOI	TCI	3353	
						E_H (kJ)	R (Å)
SH	39	24	2.593	1.590	0.472	21.36	2.784
SHM	47	43	2.647	1.593	0.466	27.03	2.772

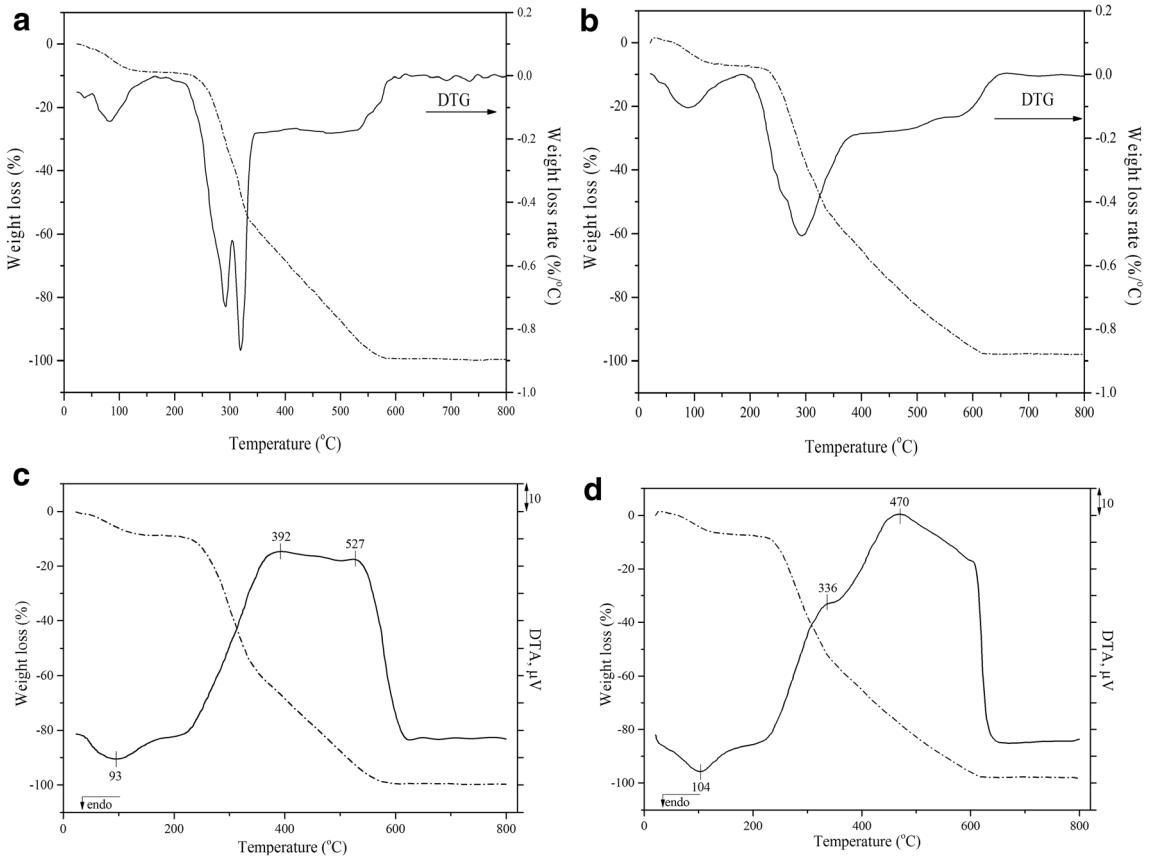

Fig. 6 TG and DTG curves of SH (**a**) and SHM (**b**) and TG and DTA curves of SH (**c**) and SHM (**d**)

water, accounting for 5.6% and 3.9% mass loss from SH and SHM, respectively. According to Jiang et al. [44], higher moisture content in SH was due to the widespread hydrogen bonding between molecules of water and more accessible hydroxyls which are present in the amorphous cellulose regions. In the second phase, the active thermal degradation process consists of hemicellulose and cellulose decompositions, falling in ranges of 220–315 °C and 315–400 °C, respectively [45]. In the hemicellulose decomposition range, SH exhibits mass losses of 34.5%, with clearly observed peak for hemicellulose at 290 °C (Fig. 6a). This temperature value is very close to one obtained for wood chips (i.e. 289 °C) by Gašparovič et al. [45]. The major peak in SH sample at 320 °C corresponds to cellulose decomposition. At this temperature peak, SH weight loss was recorded to be 47.14%. Demiral and Kul [46] have obtained results of the thermal analysis of native apricot shells which are in accordance with those presented in this paper. Alkali-treated SHM sample shows similar weight loss in the second temperature range, but the absence of hemicellulose peak degradation is obvious (Fig. 6b), clearly indicating hemicelluloses partial removal by alkali modification. Similar results were obtained by Moyo et al. [47] who observed that alkali modification of mango seed particles induced a more rapid initial decomposition of treated sample, which was a consequence of hemicellulose degradation and disappearance of the hemicellulose shoulder upon alkali treatment. Apparently, interrupted structure of modified material leads to hemicellulose and cellulose degradation at lower temperatures and production of the single wide peak at 295 °C with maximum weight loss of 35.6%. Reason for this temperature shift is the decrease of hemicellulose content after modification but also the presence of sodium ions bounded in the SHM structure which might have a catalytic effect, shifting the thermal conversion to lower temperatures [48]. For both SH and SHM samples, complex cross-linked structure and aromatic nature of lignin lead to slow decomposition which overlaps with previous thermal reactions in the range from 180 up to 900 °C, with an unclear maximum weight loss [46]. The decomposition of the organic components in the investigated samples has been finished at approximately 700 °C, and further increase of temperature up to 1000 °C did not change the ash content significantly. The final weight loss ranges from 99.5 and 97.7% for SH and SHM, respectively, where the higher amount of SHM's residual ash belongs to the presence of sodium ions incorporated in the modified biomass structure [7].

In Fig. 6c–d, DTA curves of SH and SHM samples are presented. It can be noticed that the modification process did not change the shape of TGA and DTA diagrams significantly. However, due to alkali modification, the endothermic peak

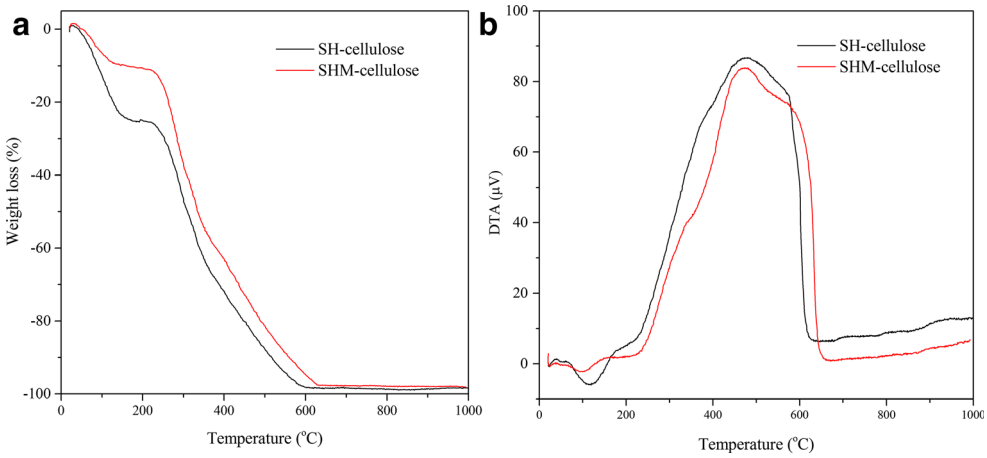

Fig. 7 Curves of cellulose isolated from SH and SHM: **a** TG and **b** DTA at 10 °C/min in air atmosphere

characteristic for moisture loss observed in SH (93 °C) had shifted toward higher temperatures, and it was observed at 104 °C in SHM sample. This shifting of the endothermic DTA peak to higher temperature might indicate an increase of the hydrophilicity of the surface of the SHM in comparison with the SH sample [49]. Conversely, exothermic DTA characteristic peaks for decomposition of organic components were shifted to lower temperatures. For the SH sample, these peaks were observed at 392 and 527 °C, while the characteristic peaks for SHM were at 336 and 470 °C. These peak shifts may be an indication that modification process has a decreasing effect on thermal stability of the SHM sample. Similar results were obtained by Krstić et al. [49] who investigated thermal stability of the carbonized saccharose sample activated by KOH.

Since the thermal stability of cellulose was found to be dependent predominantly on its crystallinity, the thermal analysis of the cellulose-rich fraction extracted from SH and SHM was performed, and the obtained results are presented in Fig. 7.

As can be seen from Fig. 7, cellulose extracted from SHM is more thermally stabile, due to the presence of cellulose II in the sample. This result is in agreement with the obtained results from XRD analysis. The observed changes can be also explained by considering the nature of supramolecular structure of cellulose, which depends on the occurrence and abundance of aggregates and/or its crystalline state [36].

Polleto et al. [38] who studied the effect of cellulose crystallinity on thermal degradation in lignocellulosic fibres showed that the thermal decomposition of cellulose shifts to higher temperatures with increasing crystalline index and crystallite size [8, 38]. Therefore, regarding the results of higher crystallinity of SHM and more compact organization of its cellulose chains, we have expected to have a positive effect on higher thermal stability of this sample compared with the native one. But the obtained results have shown that complex structure of this lignocellulosic material and modification process caused morphological changes which had a major impact on its thermal stability. Modification process induced partial hemicellulose removal, along with changes in lignin structure. Along with this, increased porosity in SHM has improved better heat transfer flux, which reflected on the shifting of characteristic peaks toward lower temperatures and enhanced thermal degradation.

4 Conclusion

The structural changes induced by alkaline treatment of apricot shells (SH) were studied, and the effect of this treatment type on the crystalline structure and thermal stability of this low-cost by-product biomass was gained. The presented results indicate that alkaline treatment has a significant effect on the surface and structural properties (especially porosity and crystallinity) of treated material. As a result of NaOH treatment, SHM sample has a more ordered crystalline structure than the native sample (SH). Modification process induces partial removal of hemicellulose and slightly changes in cellulose type, as well as disruption of lignin structure. Concerning higher crystallinity of SHM, higher *HBI* and better organization of its cellulose chains, higher thermal stability of this sample was expected. In opposite, thermal analysis revealed that described alkali modification of this material type had shifted temperature peaks toward lower values, decreasing thermal stability of SHM. This can be ascribed as increase in intra- and inter-porosity of SHM that improved heat transfer flux during combustion and enhanced thermal degradation. Everything mentioned indicates that mild conditions of alkali treatment will improve the fuel properties of this type of lignocellulosic biomass and imply SHM's possible application in energy recovery process.

Acknowledgments The authors are grateful to the Serbian Ministry of Education, Science and Technological Development for the financial support of this investigation included in the project TR 31003.

Authors' Contributions T.Š. wrote the manuscript with support from Z.L., T.Š and M.P. who carried out the experiments. J.S. and M.M. performed the XRD; FTIR, TG and DTG performed the analysis; and J.A. and A.HB. contributed to the interpretation of the results. All authors discussed the results and commented on the manuscript. All authors read and approved the manuscript.

Compliance with ethical standards

Conflict of Interest The authors declare that they have no conflict of interest.

References

1. Aldana H, Lozano FJ, Acevedo J, Mendoza A (2015) Thermogravimetric characterization and gasification of pecan nut shells. Bioresour Technol 198:634–641. https://doi.org/10.1016/j.biortech.2015.09.069
2. Wani AA, Zargar SA, Malik AH, Kashtwari M, Nazir M, Khuroo AA, Ahmad F, Dar TA (2017) Assessment of variability in morphological characters of apricot germplasm of Kashmir, India. Sci Hortic (Amsterdam) 225:630–637. https://doi.org/10.1016/j.scienta.2017.07.029
3. Ronda A, Martín-Lara MA, Calero M, Blázquez G (2015) Complete use of an agricultural waste: application of untreated and chemically treated olive stone as biosorbent of lead ions and reuse as fuel. Chem Eng Res Des 104:740–751. https://doi.org/10.1016/j.cherd.2015.10.021
4. Lopičić ZR, Stojanović MD, Marković SB, Milojković JV, Mihajlović ML, Kaluderović Radoičić TS, Kijevčanin MLJ (2019) Effects of different mechanical treatments on structural changes of lignocellulosic waste biomass and subsequent Cu(II) removal kinetics. Arab J Chem 12:4091–4103. https://doi.org/10.1016/j.arabjc.2016.04.005
5. Turk Sekulić M, Pap S, Stojanović Z, Bošković N, Radonić J, Šolević Knudsen T (2018) Efficient removal of priority, hazardous priority and emerging pollutants with Prunus armeniaca functionalized biochar from aqueous wastes: experimental optimization and modeling. Sci Total Environ 613–614:736–750. https://doi.org/10.1016/j.scitotenv.2017.09.082
6. Pap S, Šolević Knudsen T, Radonić J, Maletić S, Igić SM, Turk Sekulić M (2017) Utilization of fruit processing industry waste as green activated carbon for the treatment of heavy metals and chlorophenols contaminated water. J Clean Prod 162:958–972. https://doi.org/10.1016/j.jclepro.2017.06.083
7. Šoštarić TD, Petrović MS, Pastor FT, Lončarević DR, Petrović JT, Milojković JV, Stojanović MD (2018) Study of heavy metals biosorption on native and alkali-treated apricot shells and its application in wastewater treatment. J Mol Liq 259:340–349. https://doi.org/10.1016/j.molliq.2018.03.055
8. Carvalho MS, Virgens CF (2018) Effect of alkaline treatment on the fruit peel of Pachira aquatic Aubl.: Physico-chemical evaluation and characterization. Microchem J 143:410–415. https://doi.org/10.1016/j.microc.2018.08.021
9. Kim S, Holtzapple MT (2006) Effect of structural features on enzyme digestibility of corn stover. Bioresour Technol 97:583–591. https://doi.org/10.1016/j.biortech.2005.03.040
10. Gümüşkaya E, Usta M (2002) Crystalline structure properties of bleached and unbleached wheat straw (Triticum aestivum L.) soda-oxygen pulp. Turkish J Agric For 26:247–252. https://doi.org/10.3906/tar-0111-4
11. Poletto M, Zattera AJ, Santana RMC (2012) Structural differences between Wood species: evidence from chemical composition, FTIR spectroscopy, and thermogravimetric analysis. J Appl Polym Sci 126:336–343. https://doi.org/10.1002/app
12. Wang HM, Kessler W (2003) Removing pectin and lignin during chemical processing of hemp for textile applications. Text Res J 73:664–669
13. Kostic M, Pejic B, Skundric P (2008) Quality of chemically modified hemp fibers. Bioresour Technol 99:94–99. https://doi.org/10.1016/j.biortech.2006.11.050
14. Rouquerol J, Baron G, Denoyel R, Giesche H, Groen J, Klobes P, Levitz P, Neimark AV, Rigby S, Skudas R, Sing K, Thommes M, Unger K (2012) Liquid intrusion and alternative methods for the characterization of macroporous materials (IUPAC technical report). Pure Appl Chem 84:107–136. https://doi.org/10.1351/PAC-REP-10-11-19
15. Ben Sghaier AEO, Chaabouni Y, Msahli S, Sakli F (2012) Morphological and crystalline characterization of NaOH and NaOCl treated Agave americana L. fiber. Ind Crop Prod 36:257–266. https://doi.org/10.1016/j.indcrop.2011.09.012
16. Gan S, Zakaria S, Chen RS, Chia CH, Padzil FNM, Moosavi S (2017) Autohydrolysis processing as an alternative to enhance cellulose solubility and preparation of its regenerated bio-based materials. Mater Chem Phys 192:181–189. https://doi.org/10.1016/j.matchemphys.2017.01.012
17. Mittal A, Katahira R, Himmel ME, Johnson DK (2011) Effects of alkaline or liquid-ammonia treatment on crystalline cellulose: changes in crystalline structure and effects on enzymatic digestibility. Biotechnol Biofuels 4:1–16. https://doi.org/10.1186/1754-6834-4-41
18. Liao Z, Huang Z, Hu H, Zhang Y, Tan Y (2011) Microscopic structure and properties changes of cassava stillage residue pretreated by mechanical activation. Bioresour Technol 102:7953–7958. https://doi.org/10.1016/j.biortech.2011.05.067
19. Poletto M, Pistor V, Zeni M, Zattera AJ (2011) Crystalline properties and decomposition kinetics of cellulose fibers in wood pulp obtained by two pulping processes. Polym Degrad Stab 96:679–685. https://doi.org/10.1016/j.polymdegradstab.2010.12.007
20. Borysiak S, Doczekalska B (2008) Research into the mercerization process of beech Wood using the Waxs method. Fibres Text East Eur Nr 6(71):101–103
21. Dinand E, Vignon M, Chanzy H, Heux L (2002) Mercerization of primary wall cellulose and its implication for the conversion of cellulose I → cellulose II. Cellulose 9:7–18. https://doi.org/10.1023/A:1015877021688
22. Eriksson H (2014) Cellulose reactivity - difference between sulfite and PHK dissolving pulps 57
23. Yue Y (2011) A comparative study of cellulose I and II fibers and nanocrystals. LSU Master's Theses 764
24. Petrović M, Šoštarić T, Pezo L, Stanković S, Lačnjevac Č, Milojković J, Stojanović M (2014) Usefulness of ANN-based model for copper removal from aqueous solutions using agro industrial waste materials. Chem Ind Chem Eng Q 21:249–259. https://doi.org/10.2298/ciceq140510023p
25. Alemdar A, Sain M (2008) Isolation and characterization of nanofibers from agricultural residues - wheat straw and soy hulls. Bioresour Technol 99:1664–1671. https://doi.org/10.1016/j.biortech.2007.04.029
26. Lehto J, Louhelainen J, Kłosińska T, Drozdzek M, Alen R (2018) Characterization of alkali-extracted wood by FTIR-ATR spectroscopy. Biomass Convers Biorefinery 8:847–855. https://doi.org/10.1007/s13399-018-0327-5
27. Siqueira G, Bras J, Dufresne A (2010) Luffa cylindrica as a lignocellulosic source of fiber, microfibrillated cellulose, and cellulose nanocrystals. Bioresources 5:727–740
28. Aljoumaa K, Tabeikh H, Abboudi M (2017) Characterization of apricot kernel shells (Prunus armeniaca) by FTIR spectroscopy,

DSC and TGA. J Indian Acad Wood Sci 14:127–132. https://doi.org/10.1007/s13196-017-0197-7
29. Zhao J, Xiuwen W, Hu J, Liu Q, Shen D, Xiao R (2014) Thermal degradation of softwood lignin and hardwood lignin by TG-FTIR and Py-GC/MS. Polym Degrad Stab 108:133–138. https://doi.org/10.1016/j.polymdegradstab.2014.06.006
30. Tang PL, Hassan O, Yue CS, Abdul PM (2020) Lignin extraction from oil palm empty fruit bunch fiber (OPEFBF) via different alkaline treatments. Biomass Convers Biorefinery 10:125–138. https://doi.org/10.1007/s13399-019-00413-5
31. Rosa MF, Medeiros ES, Malmonge JA, Gregorski KS, Wood DF, Mattoso LHC, Glenn G, Orts WJ, Imam SH (2010) Cellulose nanowhiskers from coconut husk fibers: effect of preparation conditions on their thermal and morphological behavior. Carbohydr Polym 81:83–92. https://doi.org/10.1016/j.carbpol.2010.01.059
32. Pretsch E, Bühlmann P, Affolter C (2000) Structure determination of organic compounds
33. Milojković JV, Stojanović MD, Mihajlović ML, Lopičić ZR, Petrović MS, Šoštarić TD, Ristić MD (2014) Compost of aquatic weed Myriophyllum spicatum as low-cost biosorbent for selected heavy metal ions. Water Air Soil Pollut 225:1927. https://doi.org/10.1007/s11270-014-1927-8
34. Liang Q, Liu Y, Chen M, Ma L, Yang B, Li L, Liu Q (2020) Optimized preparation of activated carbon from coconut shell and municipal sludge. Mater Chem Phys 241:122327. https://doi.org/10.1016/j.matchemphys.2019.122327
35. Lupoi JS, Singh S, Parthasarathi R, Simmons BA (2015) Recent innovations in analytical methods for the qualitative and quantitative assessment of lignin. Renew Sust Energ Rev 49:871–906. https://doi.org/10.1016/j.rser.2015.04.091
36. Carrillo I, Mendonca RT, Ago M, Rojas OJ (2018) Comparative study of cellulosic components isolated from different Eucalyptus species. Cellulose 25:1011–1029. https://doi.org/10.1007/s10570-018-1653-2
37. Johar N, Ahmad I, Dufresne A (2012) Extraction, preparation and characterization of cellulose fibres and nanocrystals from rice husk. Ind Crop Prod 37:93–99. https://doi.org/10.1016/j.indcrop.2011.12.016
38. Matheus Poletto AJZ, Heitor L, Junior O (2014) Native cellulose: structure. Characterization and Thermal Properties Materials (Basel) 7:6105–6119. https://doi.org/10.3390/ma7096105
39. Chen Z, Zhang J, Huang L, Yuan Z, Li Z, Liu M (2019) Removal of Cd and Pb with biochar made from dairy manure at low temperature. J Integr Agric 18:201–210. https://doi.org/10.1016/S2095-3119(18)61987-2
40. Wei X, Wang Y, Li J, Wang F, Chang G, Fu T, Zhou W (2018) Effects of temperature on cellulose hydrogen bonds during dissolution in ionic liquid. Carbohydr Polym 201:387–391. https://doi.org/10.1016/j.carbpol.2018.08.031
41. Amador C, Martin de Juan L (2013) Tools for Chemical product design Chapter 19: Strategies for Structured Particulate Systems Design. pp 509–572
42. Lopičić ZR, Stojanović MD, Kaluđerović Radoičić TS, Milojković JV, Petrović MS, Mihajlović ML, Kijevčanin MLJ (2017) Optimization of the process of cu(II) sorption by mechanically treated Prunus persica L. - contribution to sustainability in food processing industry. J Clean Prod 156:95–105. https://doi.org/10.1016/j.jclepro.2017.04.041
43. Ronda A, Della Zassa M, Martın-Lara MA, Calero M, Canu P (2016) Combustion of a Pb (II)-loaded agrowaste used as biosorbent. J Hazard Mater:285–293. https://doi.org/10.1016/j.jhazmat.2016.01.045
44. Jiang GB, Lin ZT, Huang XY, Zheng YQ, Ren CC, Huang CK, Huang ZJ (2012) Potential biosorbent based on sugarcane bagasse modified with tetraethylenepentamine for removal of eosin Y. Int J Biol Macromol 50:707–712. https://doi.org/10.1016/j.ijbiomac.2011.12.030
45. Gašparovič L, Koreňová Z, Jelemenský Ľ (2010) Kinetic study of wood chips decomposition by TGA. Chem Pap 64:174–181. https://doi.org/10.2478/s11696-009-0109-4
46. Demiral I, Kul ŞÇ (2014) Pyrolysis of apricot kernel shell in a fixed-bed reactor: characterization of bio-oil and char. J Anal Appl Pyrolysis 107:17–24. https://doi.org/10.1016/j.jaap.2014.01.019
47. Moyo M, Pakade VE, Modise SJ (2017) Biosorption of lead(II) by chemically modified Mangifera indica seed shells: adsorbent preparation, characterization and performance assessment. Process Saf Environ Prot 111:40–51. https://doi.org/10.1016/j.psep.2017.06.007
48. Nsaful F, Collard FX, Carrier M, Görgens JF, Knoetze JH (2015) Lignocellulose pyrolysis with condensable volatiles quantification by thermogravimetric analysis - thermal desorption/gas chromatography-mass spectrometry method. J Anal Appl Pyrolysis 116:86–95. https://doi.org/10.1016/j.jaap.2015.10.002
49. Krstić SS, Kragović MM, Dodevski VM, Marinković AD, Kaluđerović BV, Žerjav G, Pintar A, Pagnacco MC, Stojmenović MD (2018) Influence of temperature and different hydroxides on properties of activated carbon prepared from saccharose. Characterization, thermal degradation kinetic and dyes removal from water solutions. Sci Sinter 50:255–273. https://doi.org/10.2298/SOS1802255K